Parametric analysis of three dimensional flow models applied to the tidal energy sites in Scotland

Accepted Manuscript

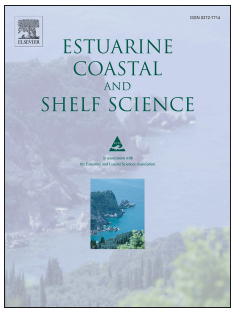

Parametric analysis of three dimensional flow models applied to the tidal energy sites in Scotland

Anas Rahman, Vengatesan Venugopal

PII: S0272-7714(17)30212-3

DOI: 10.1016/j.ecss.2017.02.027

Reference: YECSS 5404

To appear in: *Estuarine, Coastal and Shelf Science*

Received Date: 11 July 2016

Revised Date: 17 February 2017

Accepted Date: 21 February 2017

Please cite this article as: Rahman, A., Venugopal, V., Parametric analysis of three dimensional flow models applied to the tidal energy sites in Scotland, *Estuarine, Coastal and Shelf Science* (2017), doi: 10.1016/j.ecss.2017.02.027.

Parametric Analysis of Three Dimensional Flow Models Applied to the Tidal Energy Sites in Scotland

Anas RAHMAN[1] and Vengatesan VENUGOPAL[2]

Institute for Energy System, School of Engineering, The University of Edinburgh

The King's Buildings, Mayfield Road, Edinburgh EH9 3JL, United Kingdom

Corresponding author: [1]anas.rahman@ed.ac.uk / +44 (0)131 650 5612

[2]V.Venugopal@ed.ac.uk

Abstract: This paper presents a detailed parametric analysis on various input parameters of two different numerical models, namely Telemac3D and Delft3D, used for the simulation of tidal current flow at potential tidal energy sites in the Pentland Firth in Scotland. The motivation behind this work is to investigate the influence of the input parameters on the above 3D models, as the majority of past research has mainly focused on using the 2D depth-averaged flow models for this region. An extended description of the models setup, along with the utilised parameters is provided. The International Hydrographic Organisation (IHO) tidal gauges and Acoustic Doppler and Current Profiler (ADCP) measurements are used in calibrating model output to ensure the robustness of the models. Extensive parametric study on the impact of varying drag coefficients, roughness formulae and turbulence models has been investigated and reported. The results indicate that both Telemac3D and Delft3D models are able to produce excellent comparison against measured data; however, with Delft3D, the model parameters which provided higher correlation with the measured data, are found to be different from those reported in the previous literature, which could be attributed to the choice of boundary conditions and the mesh size.

Keywords: Telemac3D; Delft3D; three-dimensional; sensitivity analysis; Pentland Firth; tidal currents

1 Introduction

Studies have estimated that 25% of Europe's tidal energy is located in the Scottish waters [1], where most of this resource is concentrated in the Pentland Firth (Figure 1). Tidal current speed up to 5 m/s has been observed surging through the firth, marking this area as one of the best sites for tidal stream power generation in the world. Due to the enormous potential for generating clean and predictable tidal stream energy, the Pentland Firth and Orkney Waters (PFOW) has become the focal point in the marine renewable energy research. Between 2008 and 2010, the Crown Estate has leased several sites in the PFOW for tidal energy deployments to industries such as ScottishPower, Renewables, SSE, MeyGen and Marine Current Turbine for commercial scale developments [2]. MeyGen is currently working on the world's first and largest tidal energy farm in the Inner Sound [3], while in Shetland, Nova Innovation Ltd is currently developing the world's first community scale array of five 100KW devices [4]. Furthermore, Orkney based Scotrenewables Tidal Power is well on track to build and test the world's largest floating tidal turbine, with 2MW output capacity [4].

The Pentland Firth is a 10 km wide strait that separates the Orkney archipelago and the Scottish mainland. The region is dominated by semidiurnal tides, with primary M2 and secondary S2 tides propagating from the Atlantic Ocean on the west to the North Sea on the east. Davies et al. [5] have elaborated that the exceptional tidal current observed in the region is attributed to the large differences in the tidal amplitude observed in the west and east of the channel. In addition, this area is also notable for being extremely turbulent and thus present great challenges in obtaining field measurement data. Direct measurement poses several limitations that are essential in a hydrodynamic study. Wide spatial and long temporal data is very hard to collect since the measurement exercises are exceptionally expensive and time consuming. Therefore, accurate and robust numerical modelling is essential in validating

theoretical and analytical approaches for marine energy research. Furthermore, as PFOW is one of the most complex regions where strong tidal currents exist, the need to understand and characterise the depth-wise tidal flow behaviour becomes an important element in tidal resource prediction.

Although field measurements have been undertaken by developers, this does not cover the entire PFOW region, and the alternative is to employ a sophisticated numerical model for resource estimation. When a numerical model is used for the resource prediction purpose, the model has to be properly calibrated and validated before any longer term prediction can be performed. The objective of the calibration exercise is to select appropriate input parameters that would yield numerical output that is comparable to the measurement data. More importantly, model's calibration for any 3D simulations is a laborious process as several additional input parameters need to be considered in comparison to 2D models, and one such exercise is presented in this paper.

Several numerical models, both 2D depth-averaged and 3D models, have been utilised for hydrodynamics, morphodynamics and resource assessment studies in the Pentland Firth. Chatzirodou and Karunarathna [6] employed a 3D model to study the impacts of tidal energy extraction on sea bed morphology using the open source Delft3D software, where they found that locations favoured for tidal energy extraction (i.e. the Inner Sound channel) lie in proximity to highly sensitive sand and gravel deposits. Baston et al. [7] also utilised the Delft3D model to analyse the sensitivity of the algebraic and k-epsilon turbulence closure models, and concluded that although the models were able to satisfactorily reproduce the shape of the vertical current profile, further validation was required to provide a more 'statistically accurate' assessment on the vertical variation of current at the testing sites.

Venugopal and Nemalidinne [8] on the other hand used the commercial software, MIKE 21 and MIKE 3 to perform a 3D hydrodynamics simulation of combined wave and tidal flow in this area, where the coupled model yielded high correlation coefficients, and were able to provide a good match with ADCP measurements at different depths, despite using default values for most of the flow parameters. Easton et al. [9] also explored the flow dynamics at this location using the MIKE 21 2D hydrodynamics model. Using the quadratic friction law to calculate the energy dissipation, Easton et al. demonstrated that the mean rate of energy dissipation over two consecutive spring-neap tidal cycles in this region to be close to 5.24 GW, which agrees well with the 5.62 GW net energy flux calculated across the boundaries of the Pentland Firth.

Another 3D model, Stanford Unstructured Non-hydrostatic Terrain-following Adaptive Navier-Stokes Simulator (SUNTANS) was employed by Baston and Harris [10] in investigating the complex flow characteristic at the Pentland Firth, although the scope of this study was limited to the sensitivity analysis of the bottom friction coefficient. Furthermore, a discontinuous Galerkin, depth-averaged ADCIRC numerical model was applied by Adcock et al. [11] to explore the maximum extractable power for tidal stream resources, in which the actuator disc concept was used to model the effects of turbines on the flow. Bowyer and Marchi [12] meanwhile constructed a depth-averaged model of the Princeton Ocean Model (POM) to inspect the influence of Tidal Energy Converter (TEC) and wind on the residual flows in the channel, and concluded that the installation of large scale TECs in arrays may influence the residual circulation and possibly increase tracer (i.e. sediments or particles) deposits within the channel. Finally, Telemac2D was used by Ortiz et al. [13] to present an approach in estimating the resources in the Pentland Firth, where their results demonstrated how an oversized tidal farm may produce less power due to reduced incoming current

velocities. The study by Ortiz et al. further highlights the need to comprehend the overall effects of tidal arrays and the inherent momentum sinks, rather than just relying on the energy potential calculated from an undisturbed site evaluation.

From literature, it appears that the influence of 3D input parameters such as bottom friction, turbulence, eddy, and boundary forcing on the numerical models are yet to be thoroughly explored, discussed, and understood, especially for the Telemac3D. Moreover, most of the studies conducted in this region were completed using 2D depth averaged models, where the velocity across the water column cannot be accurately predicted. Although 3D models require more computational power to run, they are able to provide additional insights on the flow characteristic that are not possible with the 2D models, such as the turbulence component in the vertical direction, which is important to account for fluid mixing behind the turbines and dissipation of energy from the flow. Hence, the purpose of this paper is neither to examine the available resources in PFOW region nor to reproduce a resource map, as extensive studies on this subject has been conducted before, but to inspect how the values of selected model input parameters affect the results. Furthermore, since the accuracy of any numerical models are greatly dependent on open boundary conditions, input parameters and the numerical scheme, this paper is focused on applying appropriate methodology in investigating the critical parameters which are known to influence the output of 3D flow models. The novelties of this study can then be summarised as follows; Firstly, the suitability of several input parameters for the Telemac3D model is explored, since to the authors' knowledge, no 3D studies are yet to be conducted in this region using this software. Secondly, the predicted output from two distinct numerical models – Telemac3D [14] which is a finite element based numerical model, and Delft3D [15], which is a finite difference based model employing only the structured grid – are investigated and analysed.

Emphasis on the technique in constructing the 3-dimensional tidal model for the Pentland Firth is presented and elaborated in the following section. It is also in the authors' interest to explore the influence of the chosen parameters on the flow models, to see which of the two software is more adaptable and able to produce accurate numerical output (i.e. upon comparison with the measurement data). Apart from conducting the parametric study on the sensitivity of the parameters utilised for both models, this paper is also motivated by the need to comprehend the limitations and shortcomings of the two numerical software. What is more, this study presents the preliminary analysis of the efficiency of both models to produce accurate 3D flow characteristics, as the next stage of this research would involve inserting tidal turbines into the numerical models. It is hoped that this work will serve as a guideline for developing a 3D tidal model for this region by utilising the methodology presented.

2 Model Description

2.1 Telemac3D Model

Telemac3D is a finite element model that solves the Navier Stokes equations with a free surface, along with the advection-diffusion equations of salinity, temperature and other parameters. This model was developed by the National Hydraulic and Environment Laboratory (LNHE), a research and development unit under the Electricité de France (EDF) and has been made open source since July 2010. The numerical scheme is also comprised of the wind stress, heat exchange with the atmosphere, density and Coriolis effects. The 3D flow simulation (with hydrostatic assumption) is calculated by solving the following equations:

$$\frac{\partial U}{\partial x} + \frac{\partial V}{\partial y} + \frac{\partial W}{\partial z} = 0 \qquad (1)$$

$$\frac{\partial U}{\partial t} + U\frac{\partial U}{\partial x} + V\frac{\partial U}{\partial y} + W\frac{\partial U}{\partial z} = -g\frac{\partial Z_s}{\partial x} + v\Delta(U) + F_x \quad (2)$$

$$\frac{\partial V}{\partial t} + U\frac{\partial V}{\partial x} + V\frac{\partial V}{\partial y} + W\frac{\partial V}{\partial z} = -g\frac{\partial Z_s}{\partial y} + v\Delta(V) + F_y \quad (3)$$

150

151 where *U*, *V* and *W* are the three-dimensional components of the velocity, v is velocity and
152 tracer diffusion coefficient, F_x and F_y are the source terms, Z_s is the bottom depth, and g is
153 the acceleration of the gravity. The vertical velocity is then derived from the continuity
154 equation, and the hydrostatic pressure is given as:

155

$$P = P_{atm} + \rho_o g(Z_s - z) + \rho_o g\int_z^{Z_s}\frac{\Delta\rho}{\rho_o}dz \quad (4)$$

156

157 where ρ_o is the reference density, z is the vertical space component, and P_{atm} is the
158 atmospheric pressure. The second term on the right hand-side takes into account the
159 buoyancy effects due to temperature and salinity. In addition, Telemac3D also solves the
160 advection-diffusion equation in non-conservative form for a scalar quantity, *T*:

161

$$\frac{\partial T}{\partial t} + U\frac{\partial T}{\partial x} + V\frac{\partial T}{\partial y} + W\frac{\partial T}{\partial z} = v\Delta(T) + Q \quad (5)$$

162

163 In this equation, T is passive or active tracer (salinity), and Q is the tracer source of sink.
164 Telemac3D offers the choice of using either the hydrostatic or the non-hydrostatic pressure
165 code. The hydrostatic pressure code simplifies the vertical velocity (*W*) assumption, ignoring
166 the diffusion, advection and other terms. Thus, the pressure at a point is the sum of weight of
167 the water column and the atmospheric pressure at the surface. Conversely, the non-
168 hydrostatic option solves the vertical velocity equation with the additional gravity term, and

is more computationally intensive. Elaboration on theoretical aspects of Telemac3D can be found in these articles [16], [17], [18].

Telemac3D uses the same unstructured mesh as the 2D model in the horizontal direction. Grids composing of triangular facets of diverse sizes and forms enable accurate representation of complex topography within the resolution of the elements. More importantly, the non-structured mesh offers unparalleled flexibility against the structured grid, in which the grid density can be effortlessly controlled to adapt to specific applications and geometries. A more refined mesh geometry is usually applied in areas of special interest (e.g. complex coastlines, river channels and embankments), while the low resolution grid is used in locations where details are not demanded. This is essential in maximising the computational efficiency. In addition, variable thickness can also be applied in the vertical direction of the whole computational domain, depending on the required grid resolution. Several options for vertical layer mesh transformation are available in Telemac3D. In this study, the terrain following sigma (σ) transformation is implemented.

2.2 Telemac3D Model Set-up

Figure 2 illustrates the development procedure for generating a Telemac3D model. The pre-processing was performed using the Blue Kenue [19] and Fudaa PrePro (Fudaa) [20] software, which are both open source. Blue Kenue is an advanced pre and pro-processing tool developed by the National Research Council Canada for data preparation, analysis and visualisation for numerical modelling. Fudaa, on the other hand, is a tool for preparing a flow study (i.e. the steering file) developed by the Institute for Maritime and Inland Waterways (CETMEF) France. Telemac3D requires three input files; the geometry file which contains the information of the model mesh, the boundary condition file which describes the boundary

194 condition of the domain, and finally the steering file that describes the simulation
195 configuration. The first two files can be generated by using Blue Kenue, while the latter is
196 created using Fudaa.
197
198 The boundary condition file describes the domain's boundary, in which time varying values
199 (e.g. velocity, water depth and flow rate) can be specified [16], while the bathymetry
200 information is stored in the geometry file. The liquid or solid (default) boundaries of the
201 model must also be defined during the pre-processing. Conversely, the steering file contains a
202 list of keywords that are crucial for executing the simulation. It is imperative to highlight that
203 the Telemac3D uses a library that is distinctive from the Telemac2D in generating the
204 steering file, which contains the selections of computational options (physical, numerical and
205 general parameters). More importantly, the geometry and boundary conditions file generated
206 from the Blue Kenue are requested upon the creation of a new steering file.
207
208 The geometry used in the Telemac3D domain was acquired from the World Vector Shoreline
209 database, available from the shoreline toolbox in the Delft Dashboard [15]. Alternatively, the
210 GEODAS coastline extractor from the National Oceanic and Atmospheric Administration
211 (NOAA) [21] can be utilised in procuring the geometry for the domain. The geometry
212 acquired using the GEODAS tool uses Cartesian coordinate, and thus requires conversion to
213 the Universal Transverse Mercator (UTM) coordinate system as Fudaa can only accept the
214 latter coordinate system. In contrast, the shoreline extracted from the Delft Dashboard is
215 readily available in the UTM system when the appropriate study zone is selected beforehand,
216 along with the WGS 84 ellipsoid datum.
217

Upon importing the geometry into the Blue Kenue, it is imperative that the geometry lines are resampled before the mesh is generated. The purpose of resampling the lines is to allow smooth distribution of the geometry points, which is vital in producing a uniform and consistent mesh distribution for the domain. The resampling exercise is also intended in reducing the possibility of having too many points around the nodes. Apart from that, the resampling also helps to produce nearly constant areas in adjacent triangles. In the process of resampling, it is possible that the profile of the coastline will be altered, and attention must be paid in this regard to keep the shape as close to original coastline. Telemac3D system requires that the maximum number of points or elements around a node in the mesh to be less than 10. Three resampling methods are offered in Blue Kenue; the maximum distance method ensures that the distance between points do not exceed the intended value; the equal distance option allow the lines to be redrawn with equal distance between each point; and finally the segment count method will either increase or decrease the number of vertices on the lines based on the value specified by the user.

The size of the elements at the area of interest (i.e. the Pentland Firth channel) was set to a minimum distance of 200 m. Elsewhere in the domain, the edge length of the mesh was assigned to 3000 m. The edge growth ratio, which is the parameter that defines the maximum ratio between the lengths of edges at a given node, was set to the default value of 1.2. Furthermore, in an attempt to improve the numerical accuracy and to establish a fixed node within the mesh, three hard points (50 m edge length) were used as the monitoring points at the ADCPs location. The 50 m grid size imposed around the fixed nodes was deemed sufficient to properly capture the flow propagation near the monitoring points. Figure 3 shows the computational domain that was generated for use with the Telemac3D model. The domain contains 285747 nodes (inclusive of nodes in the vertical layers) and 497230

elements, with 10 equidistant sigma layers in the vertical direction, which was sufficient to represent the approximate depth where measurements were available. Additionally, the time step was set to 10 min, which was estimated using the known information (i.e. smallest mesh size, and the highest mean velocity in the study area) to meet the Courant Friedrichs Lewy (CFL) stability criterion.

For Telemac3D simulation, two sets of bathymetric data with distinctive resolution were inspected. The first was GEBCO 08 [22], a continuous terrain model for ocean and land bathymetry with a spatial resolution of 30 arc seconds. This database can be extracted by using either the GEBCO Grid Display Software [23] or from the Bathymetry's toolbox in the Delft Dashboard, both of which are available for free. The second set of the bathymetric data utilised in this study was provided by the Terawatt consortium, with a higher spatial resolution of 20 meters where the measurements were available. This bathymetric database was then combined and interpolated with the GEBCO data to provide a comprehensive coverage of the PFOW region. Open boundaries with prescribed depth (H) were applied to the liquid segment on the five sides of the domain (Figure 3), where the prescribed depth with free tracer (i.e. input from temperature and salinity are not considered) was used to supply the forcing required to drive the flow through the domain. The tidal harmonic database was derived from the Oregon State University (OSU) TOPEX/Poseidon Global Inverse Solution (TPXO), with a spatial resolution of 0.25^{o} x 0.25^{o}. The database acquired is for the sea surface elevation, and consist of the following harmonic database; eight primary (M2, S2, N2, K2, K1, O1, P1, Q1), two long periods (Mf, Mm) and 3 non-linear (M4, MS4, MN4) constituents. The open boundaries were set to be far away from the area of interest in order to reduce their influence on the solution and also to minimise numerical stability that might develop at the boundaries.

2.2.1 Boundary Conditions for Telemac3D

For the initial boundary conditions, both the TPXO satellite altimetry and constant elevation options have been put to the test and demonstrated that the pair are suitable for this application. The model simulation wrap-up time was set to three days before the intended comparison against the measured data to allow for the computation to achieve numerical stability, and the simulation period was set to 35 days [24]. 'Tidal flat' keyword was also activated in this study to take into account the areas that are periodically wet and dry during high and low tide respectively since the monitoring points were located very close to the islands of Swona and Stroma of the Pentland Firth. The choice of the numerical and physical parameters used in the models will be presented and discussed in section 3. Meteorological input (e.g. wave and wind), along with density and temperature variation were not applied as their influence on the model output was expected to be lower than the astronomical forcing. Furthermore, since the computational domain generated for Telemac3D models was not large enough for the Coriolis force to influence the computation, the models were run without the Coriolis effect. In addition to that, the default hydrostatic code was applied for all models as no substantial differences were observed when using the more computationally demanding non-hydrostatic version. The U and V-horizontal velocity components, along with the water elevation were set as the 3D output variables for the Telemac3D model.

2.3 Delft3D Model

Delft3D is a finite difference modelling suite developed by the Deltares, and consists of the flow, morphology, water quality and wave modules [25]. It applies the shallow water and Boussinesq assumptions to solve the Navier-Stokes equations, for both two and three dimensions. The numerical scheme then solves the continuity equation, momentum

293 equations, the advection-diffusion transport equations, and turbulence model. The system of
294 equations for the three-dimensional flow model are as follow:
295

$$\frac{\delta\zeta}{\delta t} + \frac{\delta\left[(\zeta + d)\overline{U}\right]}{\delta x} + \frac{\delta\left[(\zeta + d)\overline{V}\right]}{\delta y} = S \quad (6)$$

$$\frac{\delta U}{\delta t} + U\frac{\delta U}{\delta x} + V\frac{\delta U}{\delta y} + \frac{\omega}{h}\frac{\delta U}{\delta \sigma} - fV = -\frac{1}{\rho_0}P_x + F_x + M_x + \frac{1}{h^2}\frac{\delta}{\delta\sigma}\left(v_v\frac{\delta U}{\delta\sigma}\right) \quad (7)$$

$$\frac{\delta V}{\delta t} + U\frac{\delta V}{\delta x} + V\frac{\delta V}{\delta y} + \frac{\omega}{h}\frac{\delta V}{\delta \sigma} - fU = -\frac{1}{\rho_0}P_y + F_y + M_y + \frac{1}{h^2}\frac{\delta}{\delta\sigma}\left(v_v\frac{\delta V}{\delta\sigma}\right) \quad (8)$$

296
297 where S is the term due to water discharge or withdrawal, precipitation and evaporation per
298 unit area, ζ is the water level, d is the water depth in respect to a reference level (and the term
299 $(\zeta + d)$ refers to the total water depth), f is the Coriolis parameter, U and V are the
300 horizontal velocity components, ω is the vertical velocity component for sigma coordinate,
301 F_x and F_y are the horizontal Reynold's stresses, v_v refers to the eddy viscosity in vertical
302 direction, P_x and P_y are the horizontal pressure term from Boussinesq assumption, M_x and M_y
303 are the source or sink terms, and ρ_0 is the reference density.
304

305 **2.4 Delft3D Model Set-up**

306 A three-dimensional Delft3D flow model, with the Universal Transverse Mercator (UTM)
307 coordinate system was constructed using the Delft Dashboard (DDB). It consists of structured
308 computational grids that covered the whole Orkney Islands in the north of Scotland, as shown
309 in Figure 4, from 1^o 24' W – 4^o 34' W and 58^o 18' N – 59^o 37' N. Delft3D offers the choice
310 of both σ (sigma) and the Z-coordinate for generating the vertical layers in the 3D model. The
311 σ layer is known for providing accurate representation of the bathymetry, and uses less
312 computational resources since it is a terrain following model. On the contrary, the Z
313 coordinate varies in space and generates a staircase layer boundary. The option of using

either σ or Z layer grids is problem dependent. The terrain following σ layer was employed in this study since it is more suitable in modelling the physical processes near the bottom boundary layer [26]. Nonetheless, the distribution of the σ layer for the Delft3D model differs to the Telemac3D. Vertical distribution of the Delft3D layers begin at the water surface, while for Telemac3D it starts from the ocean floor. Next, as with the Telemac3D model, the TPXO 7.2 database and GEBCO 08 were applied as the boundary conditions and bathymetry for the computational domain.

Domain decomposition, which allows for local grid refinement in both horizontal and vertical direction, was applied to increase the resolution at the area of interest and also to enhance the simulation accuracy. Using this method, domains can have independent vertical grid refinement, which is not possible when using nesting [27]. Moreover, nesting technique is a one way coupling, in which there is no interaction between the domains. Nine domains were created for this work, with the largest grid resolution at 3000 m spacing for the outer domain that acts as the open boundary for the model. Although not apparent from Figure 4, two additional domains were assigned at each of the three monitoring points to allow for finer grid resolution at the measurement area. The mesh resolution was then reduced to 1000 m grid for the domain that covered the Orkney Islands. The grid was further decreased to 200 m spacing specifically for the domain that covered the Pentland Firth. As for the monitoring stations, where the Acoustic Doppler Current Profiler (ADCP) is located, a more refined mesh resolution of 22 m was employed so that the flow propagation near the point of interests can be properly captured. It is also strongly recommended to employ a maximum horizontal refinement of 1 to 5 to allow gradual transition between resolutions and avert abrupt velocity change, which may cause instability in the model. Furthermore, since Delft3D uses a structured grid, the monitoring points will be at the centre of the cell. This requires the use of

multiple domains to ensure smooth grid transitions and fine mesh density are achieved at the monitoring locations so that the distance between the monitoring and measurement points is not too great. Nevertheless, the use of multiple domain decomposition in Delft3D should be approached with caution. Aside from the suggested odd number grid refinement, users are also recommended not to place the domain boundary in a steep area to avoid potential errors caused by the large differences in depth at the adjacent cells.

Since the use of domain decomposition requires all the domain to be connected, it proves to be a hindrance especially with the presence of complex geometries and countless islands in the computational domain. Hence, an appropriate mesh density needs to be meticulously selected so that it embraces the small islands that may exist in the domain, and more crucially the grid should also be able to characterize those geometries accurately. For the purpose of this study, 10 sigma vertical layers were applied specifically to the grid that covers the Pentland Firth, while the 3000 m and 1000 m grid spacing that covers the outer domain were set to one layer (i.e. a combination of 2D outer model with a 3D high resolution model). This approach was implemented to optimise the computational resources. The Delft3D model was run with a time step of 0.1 min to satisfy the CFL condition, which should not exceed a value of ten [26]. Similar to the Telemac3D model, only astronomic forcing were included in this simulation, and default physical and numerical parameters were applied. Threshold depth was set to 0.2 m, above which the grid cell is set as wet during calculation, and k-epsilon was chosen to model the 3D turbulence. As with the Telemac3D, the simulation period was set to 35 days and the models were run without the Coriolis effect. The outputs extracted from the model were the water elevation and the U and V-horizontal velocity components.

2.4.1 Boundary Conditions for Delft3D

As displayed in Figure 4, the Delft3D domain consists of four open boundaries: North, East, South, and West. The influence of the boundary forcing on Delft3D computational domain for this region has been investigated by Rahman and Venugopal [28], and the use of water level forcing at all open boundaries has been proposed for the flow model at the Pentland Firth. In situ measurement data is critical for all numerical modelling in order to give credence to the model output. Acoustic Doppler Current Profiler (ADCP) data supplied by the EPSRC Terawatt project [29] is used to validate the numerical models at three sites. Nonetheless, any errors or uncertainties that may be present in the ADCP data are not known to the authors, and it is assumed that the provided measurement data has undergone quality control procedure. ADCP data is very useful for 3D hydrodynamics modelling as it supplies data on flow velocities throughout the water column. The locations of these devices at the Pentland Firth are given in Figure 1. The acquired data offered a measurement time step of every 10 min at 4 m intervals through the water column, with the deepest measurement approximately 5 m above the ocean floor. Details of the field data are given in Table I.

Water surface elevation measurement can be obtained via tidal gauges. Delft3D Dashboard software incorporates a worldwide tide stations database, together with the stations' astronomical components within the software's tide station toolbox. It is worth noting that the measurement data available from the tide stations include both astronomical and meteorological input, while the general models utilised in this study only consider the astronomical input.

The first step in validating the numerical model is to compare the predicted water surface elevation with the available tidal gauge database in the computational domain. This

388 procedure was performed to check the suitability of the chosen boundary conditions in
389 simulating the hydrodynamics of the study. The comparison of the water surface elevation
390 between the Telemac3D model and measured data was conducted at two tidal gauges;
391 Scrabster IHO and Wick IHO. Figure 5 produced from the Telemac3D model shows an
392 excellent comparison of the water elevation between the model output and the two tidal
393 gauges. The comparisons shown here covered a full spring tidal cycle from 16/09/01-
394 26/09/01, and demonstrated that the open boundary with the prescribed water level forcing is
395 highly suitable for the hydrodynamics application in this computational domain. The
396 simulations were also run for 35 days.
397
398 For Delft3D calibration, following the procedure set by Rahman and Venugopal [28], two
399 different models were created as part of the calibration process to inspect the influence of the
400 boundary on the computational domain, as summarised in Table II. The first model (denoted
401 as Mix BC) employed a mixture of current and water level forcing for the boundaries, in
402 which the current boundary condition was set for only the west segment. On the other hand,
403 the second model (denoted as Water Level BC) used water level for all four open boundaries.
404
405 As with Telemac3D, water elevations from the Delft3D models were compared with the tidal
406 gauges at Wick IHO and Sule Skerry IHO and are represented in Figure 6. As evident from
407 this figure, the predicted water surface elevation using the mix boundary (Mix BC) shows
408 poor correlation against the tidal gauges at both locations, indicating that this boundary
409 condition is ill-suited for this application and region. Two possible reasons may contribute to
410 this observation. Firstly, it could be due to the inability of the current data from the tidal
411 global model to be accurately resolved in the area of study due to the huge interval (i.e.
412 3000m) between the nodes along the open boundary. Although refining the grid density of

413 the outer domain may improve the numerical output of the Mix BC model, it is not within the
414 scope of the present study. Secondly, currents may also be affected by waves and other
415 oceanography processes. Since the present study did not consider the influence of waves, it
416 might be plausible that the poor result shown by the Mix BC model was caused by the
417 absence of wave propagation at the open boundaries. On the other hand, the Water Level BC
418 model displayed an excellent match with the measured data at the two sites, since water
419 elevation is highly predictable. The influence of the selected boundaries on the model's
420 hydrodynamics will be presented in the following section.
421

422 ## 3 Sensitivity analysis on Telemac3D models

423 Several sets of performance indices were utilised in comparing the measured data with the
424 numerical models. Pearson's correlation coefficient, *r*, is a measure of the strength of the
425 linear relationship between two data sets. An *r* value closer to 1.0 indicates a strong
426 relationship between variables. The difference between predicted and observed values can be
427 evaluated using Root Mean Square Error (*RMSE*), where a smaller value indicates good
428 model performance. In addition to this, scatter index (*SI*), which is the root mean square
429 difference between the model and the mean of the field data, was used in the analysis.
430

431 The general set up for the Telemac3D model used in this study was as follows: the law of
432 bottom friction was set to the Chezy formulation; the coefficient for both horizontal and
433 vertical diffusion of velocities were set to the default value of 1.0×10^{-6}; the Coriolis force
434 was not included in the model; the time step for the output file was set at 10 min interval; and
435 the mixing length model using the Prandtl's theory and the constant viscosity (default option)
436 were set as the vertical and horizontal turbulence models respectively. The results were then

compared at three different depths; near the water surface (7 m), at the middle of the water column (39 m) and close to the ocean floor (65 m-71 m).

3.1 Bottom roughness

Bottom friction has proven to be an important and sensitive parameter in tidal modelling. Several drag coefficients, Cd, have been suggested for the Pentland Firth model by previous studies. Salter [30] has proposed a value of 0.0086 based on the paper by Campbell et al. [31], while Baston et al. [7] used a roughness value of 0.0025 for their 3D models. Chatzirodou and Karunarathna [6] on the other hand utilised a constant Chezy value of 50 in their study. Nevertheless, the optimal roughness value for the study area using Telemac3D models was found to be 0.005 (Rahman and Venugopal [28]), which is consistent with the one proposed by Easton et al. [11] who used the MIKE 21 model. Telemac3D offers numerous friction laws to be used for the flow model, namely Haaland, Chezy, Strickler, Manning and Nikuradse [32]. Nonetheless, three constant Chezy values of 44, 63 and 34 which corresponded to bed friction of Cd = 0.005, Cd = 0.0025, Cd = 0.086 were tested for this comparative study.

Figures 7 and 8 show the comparison of several roughness values as proposed in the literature against the measured ADCP data, for both the U and V-velocity components at the three sites. The figures display the results obtained during the spring tide from 16 - 21/09/2001 for Site 1 and Site 3, and 21 - 26/09/2001 for Site 2 since the available field data for this location starts from 19 September 2001. Although the results for both neap and spring tidal cycle are available, only the spring tide outputs are shown here for clarity. Note that that the neap tide results also produced excellent comparison against the measurement data.

Figure 9 displays the scatter plots and performance indices (obtained from the same data presented in Figures 7 and 8) for the three bed frictions coefficients inspected in this study. It can be seen from the performance indices in Figure 9 that Cd = 0.005 consistently produced the highest r values, the lowest *RMSE* and *SI* values amongst the roughness values, indicating great correlation between the predicted and measured values. Nonetheless, although the predicted velocity using Chezy 44 (corresponds to Cd = 0.005) yielded excellent comparison against the measurement data for the three monitoring points, random scatters were apparent for Site 1 as displayed in Figures 8 and 9. Further inspection reveals that this was caused by the random fluctuation in the V-velocity component at this site. Also this could be due to the fact that the predominant flow is in U-component direction. Complex turbulence and large eddy circulation, due to the uneven bed structure in this region, could have been attributed as possible causes of this phenomenon, in which the hydrostatic solver utilised in this study may not have been able to sufficiently resolve the turbulence fluctuations. These results are essentially similar to the one produced by Venugopal and Nemalidinne [8] who used the MIKE 3 model, where high and erratic V-velocity fluctuations were also demonstrated by the ADCP data at Site 1.

3.2 Bathymetric Input

The accuracy of a tidal model is highly influenced by the quality of the bathymetry input [33]. Bathymetry data provides the depths and topography of the underwater terrain, and the term resolution is used to describe the level of its details. Obtaining detailed bathymetry and topographical information can be potentially very expensive, although a number of free database are available. A comparative study between two different sets of bathymetric data was conducted to examine the impact they may have on the numerical model. The first bathymetry was from the GEBCO 08 with a spatial resolution of 30 arc seconds, and the

second was a high 20-meter-resolution dataset supplied by the Terawatt project. Interestingly, no noticeable differences (in terms of the predicted velocity) are observed between the two bathymetric data at the three monitoring stations. However, it is worth highlighting, that detailed bathymetry is crucial when turbines are incorporated in the simulation as it may influence the hydrodynamics in the region where the devices are deployed.

3.3 Nikuradse roughness formula

The pioneering work on understanding the effect of roughness on pressure drop was done by Nikuradse [34] who carried out experiments on fluid flow in smooth and rough pipes. His study demonstrated that the characteristics of the friction factor were different for laminar and turbulent flow. In the laminar region, the roughness was shown to have very little influence, however in the turbulent region, roughness played a major role. In numerical modelling, Nikuradse roughness has been used in some of the flow models (e.g. MIKE 3) and the influence of this parameter has also been tested with Telemac3D. Three models with distinct roughness values were tested using the Nikuradse formula, as presented in Figure 10. Friction coefficient of 0.001 (smooth mud), 0.1, and 1.0 (sand) using the Nikuradse formula were simulated, which produced scatter plots that were rather poor. The models severely underestimated the current speed at Site 1 and Site 3, a *RMSE* value as high as 1.49 was observed at Site 1. Reasonable performance indices, however, were observed at Site 2 though the models again under predicted the current speed near the sea bed. Overall, the use of Nikuradse roughness formula for the bed friction resulted in substantial velocity reduction against the ADCP data.

These results seem to infer that the general numerical, physical or general parameters applied to the models are not compatible with the Nikuradse roughness option. In contrast with the

Chezy and Manning bed friction, Nikuradse formula assumes a logarithmic profile near the bottom, and thus some refinement is needed for the vertical layers. Since this work employed the equidistant layer, it then seems plausible that the law of bottom friction using the Nikuradse formula is not compatible with the model. In contrast, Strickler-based equations such as the Manning and Chezy roughness formulae are more suited for models applying the equidistant layer.

3.4 Horizontal Turbulence Model

Telemac3D offers four options in defining the horizontal turbulence model, namely constant viscosity, the k-epsilon model, Smagorinsky and also the k-omega model. Two of the turbulence models, the constant viscosity and the Smagorinsky, were applied to the Telemac3D models to assess their influence on the flow. The constant viscosity (default option in Telemac3D system) is the simplest turbulence model, and prescribes constant turbulent viscosities (both in the vertical and horizontal direction) throughout the domain. The Smagorinsky model, on the other hand, is recommended for simulations that involve highly non-linear flow. In both cases, the coefficient for both horizontal and vertical diffusion of velocities were set to their default value of $1x10^{-6}$. A comparative study conducted on the two horizontal turbulence models indicated that there were no apparent differences between the two outputs. It may be reasonable to assume that the flow in the Pentland Firth is highly turbulent and non-linear since the use of Smagorinsky model matched the measured data well. Aside from that, the attempt to use k-epsilon model in this study was unsuccessful and will be explored in future work.

Next, the influence of the viscosity coefficients was investigated, where the selected coefficient values were expected to have some influence on the eddies and recirculation.

These parameters are used to control the size and shape of the recirculation of eddies, where small size eddies can be dissipated using a small coefficient, while large sized recirculation can be reduced using a higher coefficient value [16]. Three values ($k = 1x10^{-6}$ (default), $k = 0.01$, $k = 1$), for the coefficient for horizontal diffusion of velocities, were selected and applied for the model using the constant viscosity. Although not shown in this paper, the performance indices from this exercise suggested that the models are unaffected by the value of the horizontal viscosity coefficients, which is somewhat unexpected. This result seems to imply that the three coefficient values utilised in the models may have greatly dissipated the eddies to be smaller than a two mesh cell [16], indicating the presence of a highly turbulent flow in the area.

3.5 Vertical Turbulence Model

There are four models to choose from upon selecting the mixing length as the vertical turbulence model; the Prandtl model (default value) is suited for barotropic simulation such as tidal flows; Nezu and Nakagawa; and also Quentin and Tsanis models, which offer a good representation of wind drift. All four mixing length models were investigated in this study, where the models were coupled together with constant viscosity and also Smagorinsky as the horizontal turbulence models. It is interesting to see that the four mixing length models compare well against each other, and the difference between the models are almost negligible. Furthermore, the use of either the constant viscosity or the Smagorinsky option as the horizontal turbulence model shows no noticeable influence on the output, which agrees well with previous finding in section 3.4.

4 Parametric Study on Delft3D models

For the Delft3D model setup, WGS 84 / UTM zone 30N was set as the coordinate system and GEBCO 08 bathymetry was employed. The roughness formula was set to the Chezy formulation unless stated otherwise, and default values were utilised for both the horizontal and vertical viscosity and diffusivity. Next, the history time step of 10 min was applied while the meteorological input was not considered. The results were then compared at three different depths, the same as for the Telemac3D model, e.g. near the water surface (7 m), at the middle of the water column (39 m) and close to the ocean floor (65 m-71 m). The parametric study of the turbulence closure model was not performed since it had been studied by Baston et al. [7].

4.1 Bottom roughness

Under the physical parameters tab in the Delft3D Dashboard, several options for the roughness formula are available, which are the Manning, White-Colebrook, Chezy and Z_o. Chezy was selected as the default roughness formula and applied to the Delft3D models. Apart from the bed friction values employed previously for the Telemac3D models, an additional roughness coefficient, shown here in Table III, was tested to examine its influence on the output since Delft3D allows for variable roughness coefficient to be applied for the U and V-velocity components. Model-Water Level BC (from Table II) was used in this setup. Figure 11 and 12 illustrate the U and V-velocity components of the applied roughness values when compared against the measured data, while Table IV presents the performance indices of the bed friction values (obtained from the same data) tested on the Delft3D model. At Site 1, a high *RMSE* value and very low correlation coefficient can be seen from performance indices, though high V-velocity fluctuation was attributed to the poor results. Site 2, nonetheless, showed a better comparison where high r values were observed at all depths.

585 Overall, it can then be concluded that Cd = 0.0086 (Chezy 34) is the optimal bed friction
586 value to be applied for the Delft3D flow model for this study area, based on the calculated
587 performance indices. However, it is compelling to see that this result appears to contradict the
588 values proposed by both Baston et al. [7] and Chatzirodou and Karunarathna [6], where lower
589 bed friction coefficients of Cd = 0.0025 and constant Chezy value of 50 were applied
590 respectively in each of their studies using the same numerical software. These differences
591 could be due to the size of the domain and also the mesh resolution that were utilised in their
592 models. For instance, Baston et al. employed a shelf-scale domain that was significantly
593 larger than the one used in this study, along with a finer grid density (2km x 2km) for the
594 outer region.
595

596 **4.2 Boundary Forcing**

597 Most flow models would apply either the Water Level or Current, or the combination of both
598 as the boundary forcing. In addition to that, the reflection coefficient, alpha, should be chosen
599 so that they are sufficiently large enough to damp the short waves introduced at the start of
600 the simulation. An alpha value of 1000 was applied to the model to reduce reflections at the
601 open boundaries, and the wave from propagating back into the domain as a disturbance. The
602 influence of the boundary forcing on the domain was examined using two models (Mix BC
603 and Water Level BC) with distinctive open boundaries as presented in Section 2.4.1. The
604 validation process demonstrated that Water Level BC model showed excellent comparison
605 for the water surface elevation against the tidal gauges, and thus considered as the suitable
606 boundary forcing for this model. Nonetheless, the performance indices calculated in Table V
607 have generated some interesting observations for the current speed using the two models
608 (with Cd = 0.0086). At Site 1 and Site 3, Mix BC model showed slightly better agreement
609 with *r*, *RMSE* and *SI* values compared to Water Level BC model for the three depths. Then

for Site 2, the *r* values for both models are very close to one another, while the *RMSE* and *SI* for Water level BC model are slightly better than Mix BC model. The results seem to imply that there is not much difference between the two models when direct velocity comparison are conducted. However, as noticed from the calibration procedure in Section 2.4.1, the all water level boundary forcing showed the best fit against tidal gauges, and thus best suited for hydrodynamics modelling in this region. It is evident from this analysis that proper calibration and validation are essential in producing a flow model that is both robust and also accurate.

4.3 Bottom Friction Modelling by Manning and Chezy Formula

As with Telemac3D, two of the most commonly used formulation for the bottom roughness, Chezy and Manning were examined to inspect their influence on the numerical model. Constant Chezy and Manning roughness values of 34 ($m^{1/2}s^{-1}$) and 0.06 ($m^{1/3}s^{-1}$) respectively, both of which both corresponded to Cd = 0.0086, were utilised for this comparison. Interestingly, Table VI shows contrasting output between the two models, where the computed performance indices for the Manning formula were found to be considerably lower than the Chezy. The Chezy model outperformed the Manning's at all sites and depths, where large scatter was apparent for the Manning output. Moreover, although both Telemac3D and Delft3D use the same equation in calculating the bed friction, only Telemac3D shows good agreement in result for both Chezy and Manning formulation. The reason for this observation is not very clear to the authors. In order to verify the scatter plots, the velocity components of both models at the mid water column (depth = 39 m) are presented in Figure 13. It can clearly be seen from the figure that even though the velocities were in phase, the Manning formula somehow produced a noticeably higher amplitude that contained double peaks. In an effort to prove that the result is not due to the miscalculation or error in modelling, another set of

performance indices for the model using the variable roughness values (as shown in Table III) are presented in Table VII. Despite using a different bed coefficient, once again the same occurrence was noticed for the model utilising the Manning formula. It could be speculated that the Manning roughness formula is not suitable to be used in this location under the current setting. Extensive calibration is therefore highly recommended before the Manning roughness formula is applied to the Delft3D flow model for this region.

5 Discussion

As noted above, the results from both Telemac3D and Delft3D models illustrate that the physical and numerical parameters used for the simulations worked well. The use of unstructured mesh for the Telemac3D offers an excellent tool for users to accurately model the domain geometries. Delft3D on the other hand offers an easy to use interface to create and run a model. However, there are some inherent limitations with the current release of Delft3D Dashboard (e.g. choice of unstructured mesh). Currently the option of Flexible Mesh is yet to be made open source in Delft3D, and thus users are resigned to using a structured mesh for their model. As discussed in previous sections, a structured mesh posed a problem in representing geometry with complex coastlines along with the presence of islands in the domain. Nonetheless, since the area of interest in this study is significantly deep, and the models are run without the waves input, the shoreline may have little to no influence on the predicted model output. Besides, the option for physical, numerical and general parameters offered in the Dashboard are also not as extensive as the Telemac3D module. Nonetheless, data extraction for Delft3D model is extremely easy and fast, since the use of monitoring points eliminate the need to store data for all the points in the domain.

Although several hydrodynamics studies have been done at the Pentland Firth using various numerical models, detailed model set up and the parametric analysis were neither shown nor properly discussed. Due to that reason, this work was conducted to explore the influence of key parameters such as the boundary forcing and roughness formula on the model. In essence, although both Telemac3D and Delft3D produced excellent agreement with the measured data, some variations are still to be expected. Both Telemac3D and Delft3D flow models used here only considered astronomic forcing. In contrast, the ADCP data includes both the astronomical and meteorological phenomena. In future work, meteorological input shall be included in the model and spatially varying roughness coefficient may be tested. The domain of the model would also be enlarged to include the continental shelf for conducting the resource assessment analysis. In addition to that, to incorporate tidal energy converters into the model, the high resolution bathymetry data will be utilised in future simulations to accurately represent the topography at the deployment area.

6 Conclusion

Since the majority of numerical models employed for hydrodynamics and resource assessment studies at the PFOW were conducted using 2D depth-averaged models, there is a gap that needs to be addressed to further understand the characteristic of 3D models, more so at an area with a highly turbulent flow like the Pentland Firth. Thus appropriate methods in developing a 3D tidal flow model for the PFOW using both Telemac3D and Delft3D numerical models, were thoroughly highlighted since they were not described in detail by previous studies. Great care was taken to ensure the robustness of the models, and the predicted values were validated against the observed data to give confidence to the model. The physical, numerical and general parameters utilised in the models were elaborated in detail, since the input required for a 3D model differs remarkably from the 2D model. The

parametric study was conducted to examine the influence of key simulation parameters on the numerical output, and the performance indices were utilised in comparing the predicted and measured data.

Of the three tested bed friction values for Telemac3D models, Cd = 0.005 produced the best results and can be parameterised by using both Chezy and Manning formulation. The use of Nikuradse formulation as the bottom friction was not suitable in this study since it required highly refined vertical layers, especially near the sea bottom. The findings also demonstrated that the model output was unaffected when varying the values of the horizontal diffusion of velocities, indicating the presence of a highly turbulent flow in the area of interest. Additionally, four distinct mixing length models were investigated on Telemac3D, and the difference between the models were found to be negligible.

Correspondingly, the use of Water Level BC as the boundary forcing in Delft3D produced the best agreement with the observed data. Of all the roughness values tested on Delft3D model, Cd = 0.0086 produced the best agreement with the measured data in this study. Moreover, the observed difference in the Cd values from the literature could be attributed to the choice of boundary conditions and the grid size, which may have an influence on the numerical model. Excellent correlation between the predicted and measured data was observed when Chezy formula was applied. Conversely, models utilising Manning formulation displayed a highly scattered plot, suggesting that it was not suitable to be adopted in this study. Interestingly, even though the drag coefficient definition (or mathematical meaning of the coefficient) is same in both the models, the fact that best results were obtained for different Cd values indicates that the drag coefficient is also dependent on other model input parameters (e.g. spatial resolution and bathymetry data). However, this dependency is

difficult to isolate, as both models were constructed differently (e.g. unstructured mesh in Telemac3D and structured mesh in Delft3D). In essence, it can be concluded that each of the numerical models is unique and non-identical and that thorough calibration and validation is required to ensure the validity of the numerical output.

To summarise, the present study highlighted the preliminary analysis of the capability and efficiency of both numerical models (Telemac3D and Delft3D) to produce accurate 3D flow characteristics. This work was carried out since the influence of the input parameters for 3D hydrodynamics models are yet to be thoroughly examined and explored, specifically for the PFOW region. Future work will involve implementing tidal devices into the numerical models and assessing their impacts on the surrounding environment. It is hoped that this work may be used as a guideline for developing a 3D tidal model for this region by utilising the methodology presented.

Acknowledgements

The first author would like to extend sincere grateful thanks for the funding provided by the Ministry of Higher Education, Malaysia and also the Universiti Malaysia Perlis (UniMAP) which enable this research to be carried out. Also the authors are grateful for the ADCP data supplied by the EPSRC funded Terawatt project (EP/J010170/1).

References

[1] The Scottish Government, “Energy in Scotland: Get the facts,” 2014. [Online]. Available: http://www.gov.scot/Topics/Business-Industry/Energy/Facts. [Accessed: 06-Apr-2016].

[2] The Crown Estate, “Wave and tidal energy in the Pentland Firth and Orkney waters - Delivering the first phases of projects,” 2013.

[3] MeyGen Ltd, “MeyGen Phase 1 EIA Scoping Document.” 2011.

[4] RenewableUK, “Wave & Tidal Energy,” 2016. [Online]. Available:

http://www.renewableuk.com/en/renewable-energy/wave-and-tidal/. [Accessed: 06-Apr-2016].

[5] A. M. Davies, S. C. M. Kwong, and J. C. Lee, "A Detailed Comparison of a Range of Three-Dimensional Models of the M2 Tide in the Faeroe – Shetland Channel and Northern North Sea," *J. Phys. Oceanogr.*, vol. 31, no. 1995, pp. 1747–1763, 2001.

[6] A. Chatzirodou, H. Karunarathna, S. Mainland, P. Firth, and S. Park, "Impacts of tidal energy extraction on sea bed morphology," *Coast. Eng.*, 2014.

[7] S. Baston, R. E. Harris, D. K. Woolf, R. A. Hiley, and J. C. Side, "Sensitivity Analysis of the Turbulence Closure Models in the Assessment of Tidal Energy Resource in Orkney," in *10th European Wave and Tidal Energy Conference (EWTEC)*, 2013.

[8] V. Venugopal and R. Nemalidinne, "Marine Energy Resource Assessment for Orkney Waters with a Coupled Wave and Tidal Flow Model," in *33rd International Conference on Ocean, Offshore and Arctic Engineering (OMAE2014)*, 2014.

[9] M. C. Easton, D. K. Woolf, and P. a. Bowyer, "The dynamics of an energetic tidal channel, the Pentland Firth, Scotland," *Cont. Shelf Res.*, vol. 48, pp. 50–60, Oct. 2012.

[10] S. Baston and R. E. Harris, "Modelling the Hydrodynamic Characteristics of Tidal Flow in the Pentland Firth," in *9th European Wave and Tidal Energy Conference (EWTEC)*, 2010.

[11] T. A. A. Adcock, S. Draper, G. T. Houlsby, A. G. L. Borthwick, and S. Serhadlıoğlu, "The available power from tidal stream turbines in the Pentland Firth," *Proc. R. Soc. A Math. Phys. Eng. Sci.* , vol. 469, no. 2157, Sep. 2013.

[12] P. Bowyer and G. Marchi, "Tidal Residual flows in the Pentland Firth," in *9th European Wave and Tidal Energy Conference (EWTEC)*, 2011.

[13] A. Pérez-Ortiz, J. Pescatore, and I. Bryden, "A Systematic Approach to Undertake Tidal Energy Resource Assessment with Telemac-2D," in *10th European Wave and Tidal Energy Conference (EWTEC)*, 2013.

[14] EDF, "TELEMAC-MASCARET." [Online]. Available: http://www.opentelemac.org/.

[15] Deltares, "Delft3D Open Source Community," 2014. [Online]. Available: http://oss.deltares.nl/web/delft3d.

[16] EDF, "TELEMAC-3D Operating Manual," no. March. 2013.

[17] J. M. Hervouet and J. Jankowski, "Comparing numerical simulations of free surface flows using non-hydrostatic Navier-Stokes and Boussinesq equations," 1999.

[18] Telemac, "TELEMAC-3D CODE," no. December. 2007.

[19] M. Serrer, "Blue Kenue: Software for the Hydraulic Modellers," 2012. [Online]. Available: http://www.nrc-cnrc.gc.ca/eng/solutions/advisory/blue_kenue_index.html.

[20] N. Clavreul, "Fudaa PreProcessor," 2012. [Online]. Available: http://prepro.fudaa.fr/index.en.php.

[21] National Oceanic and Atmospheric Administration (NOAA), "GEODAS-NG Desktop Software," 2014. [Online]. Available: http://www.ngdc.noaa.gov/mgg/geodas/geodas.html.

[22] International Hydrographic Organization (IHO), "The General Bathymetric Chart of the Oceans (GEBCO)," 2015. [Online]. Available: http://www.gebco.net/. [Accessed: 01-Apr-2015].

[23] British Oceanographic Data Centre (BODC), “GEBCO Grid Display Software,” 2009. [Online]. Available: http://www.gebco.net/about_us/news_and_events/grid_display_version_211.html.

[24] C. Legrand, “Assessment of Tidal Energy Resource,” 2009.

[25] G. R. Lesser, J. a. Roelvink, J. a. T. M. van Kester, and G. S. Stelling, “Development and validation of a three-dimensional morphological model,” *Coast. Eng.*, vol. 51, no. 8–9, pp. 883–915, Oct. 2004.

[26] M. Bijvelds, “Numerical Modelling of Estuarine Flow Over Steep Topography,” Delft University, 2001.

[27] Deltares, “Delft3D Flow User Manual.” 2014.

[28] A. Rahman and V. Venugopal, “Inter-Comparison of 3D Tidal Flow Models Applied To Orkney Islands and Pentland Firth,” in *11th European Wave and Tidal Energy Conference (EWTEC 2015)*, 2015, p. 08D4-2-1.

[29] “TeraWatt Consortium.” [Online]. Available: http://www.icit.hw.ac.uk/research/terawatt.htm.

[30] S. H. Salter, “Correcting the Under-estimate of the Tidal-Stream Resource of the Pentland Firth,” in *Proceedings of the 8th European Wave and Tidal Energy Conference*, 2009.

[31] A. R. Campbell, J. H. Simpson, and G. L. Allen, “The Dynamical Balance of Flow in the Menai Strait,” *Coast. Shelf Sci. Estuar.*, no. February 1997, pp. 449–455, 1998.

[32] J. M. Hervouet, *Hydrodynamics of Free Surface Flows: Modelling with the finite element method*. 2007.

[33] V. Venugopal, T. Davey, H. Smith, G. Smith, F. Girard, L. Cavaleri, L. Bertotti, and J. Lawrence, “Application of Numerical Models - EquiMAR Deliverable D2.3,” 2010.

[34] J. Nikuradse, “Laws of Flow in Rough Pipes (Stromungsgesetze in Rauen Rohren), VDI-Forschungsheft) vol. 361, 1933. Beilage zu: Forschung auf dem Gebiete des Ingenieurwesens, Ausgabe B Band 4; English Translation NACA Tech. Mem. 1292,” 1950.

Table I: Details on the ADCP measurement data

ADCP	Coordinate	Depth	Measurement data
Site 1	58° 43' 34.00" N 3° 14' 11.01" W	82 m	14/9/2001 - 16/10/2001
Site 2	58° 43' 1.02" N 3° 5' 9.02" W	80 m	19/9/2001 - 20/10/2001
Site 3	58° 40' 13.02" N 2° 58' 35.03" W	71 m	15/9/2001 - 14/10/2001

Table II: The boundary conditions applied to the Delft3D models

Mix BC	Water Level BC
West : Current	West : Water Level
North : Water Level	North : Water Level
East : Water Level	East : Water Level
South : Water Level	South : Water Level

Table III: Variable roughness coefficient applied to the Delft3D model

Site	U velocity	Cd	V velocity	Cd
1	Chezy 50	0.0039	Chezy 20	0.0245
2	Chezy 60	0.0027	Chezy 55	0.0032
3	Chezy 60	0.0027	Chezy 50	0.0039

Table IV: Performance indices of the tested bed friction values between the observed and predicted velocity magnitude at three distinct depths for Delft3D models.

		SITE 1			SITE 2			SITE 3		
Depth	**Cd**	**r**	**RMSE**	**SI**	**r**	**RMSE**	**SI**	**r**	**RMSE**	**SI**
7m	**0.0027-0.0032**	0.793	0.696	0.348	0.921	0.438	0.260	0.879	0.518	0.254
	0.0050	0.790	0.687	0.347	0.933	0.426	0.257	0.888	0.520	0.264
	0.0025	0.779	0.722	0.361	0.925	0.429	0.254	0.871	0.537	0.264
	0.0086	0.781	0.687	0.347	0.935	0.416	0.249	0.900	0.525	0.274
39m	**0.0027-0.0032**	0.700	0.852	0.430	0.926	0.380	0.225	0.863	0.514	0.252
	0.0050	0.707	0.822	0.417	0.937	0.360	0.217	0.876	0.480	0.244
	0.0025	0.685	0.872	0.436	0.930	0.371	0.220	0.855	0.536	0.263
	0.0086	0.723	0.720	0.384	0.941	0.368	0.229	0.893	0.463	0.247
71m (65m)	**0.0027-0.0032**	0.615	0.766	0.485	0.911	0.669	0.416	0.750	0.745	0.407
	0.0050	0.638	0.653	0.442	0.922	0.368	0.281	0.788	0.494	0.316
	0.0025	0.587	1.071	0.572	0.917	0.684	0.420	0.770	0.882	0.441
	0.0086	0.638	0.496	0.394	0.934	0.216	0.199	0.807	0.410	0.322

Table V: Performance indices of the boundary forcing analysis between the observed and predicted current speed at three distinct depths for Delft3D models.

		SITE 1			SITE 2			SITE 3		
Depth	**Boundary forcing**	**r**	**RMSE**	**SI**	**r**	**RMSE**	**SI**	**r**	**RMSE**	**SI**
7m	**Water level**	0.781	0.687	0.347	0.935	0.416	0.249	0.900	0.525	0.274
	Water level and current	0.795	0.621	0.334	0.941	0.485	0.313	0.903	0.545	0.294
39m	**Water level**	0.723	0.720	0.384	0.941	0.368	0.229	0.893	0.463	0.247
	Water level and current	0.742	0.626	0.355	0.946	0.429	0.287	0.891	0.448	0.248
71m (65m)	**Water level**	0.638	0.496	0.394	0.934	0.216	0.199	0.807	0.410	0.322
	Water level and current	0.648	0.456	0.385	0.932	0.234	0.232	0.795	0.417	0.339

Table VI: Statistical results of the tested bottom roughness formulation between the observed and predicted velocity magnitude at three distinct depths for Delft3D models. The bed friction was fixed to Cd = 0.0086.

		SITE 1			SITE 2			SITE 3		
Depth	**Roughness formula**	**r**	**RMSE**	**SI**	**r**	**RMSE**	**SI**	**r**	**RMSE**	**SI**
7m	**Chezy**	0.781	0.687	0.347	0.935	0.416	0.249	0.900	0.525	0.274
	Manning	0.695	1.098	0.453	0.869	0.544	0.282	0.795	0.729	0.332
39m	**Chezy**	0.723	0.720	0.384	0.941	0.368	0.229	0.893	0.463	0.247
	Manning	0.576	1.130	0.505	0.881	0.492	0.271	0.793	0.701	0.336
71m (65m)	**Chezy**	0.638	0.496	0.394	0.934	0.216	0.199	0.807	0.410	0.322
	Manning	0.483	0.751	0.498	0.879	0.342	0.281	0.744	0.491	0.349

Table VII: Statistical results of the tested bottom roughness formulation between the observed and predicted velocity magnitude at three distinct depths for Delft3D models. The bed friction was set using variable roughness coefficient.

		SITE 1			SITE 2			SITE 3		
Depth	**Roughness formula**	**r**	**RMSE**	**SI**	**r**	**RMSE**	**SI**	**r**	**RMSE**	**SI**
7m	**Chezy**	0.793	0.696	0.348	0.921	0.438	0.260	0.879	0.518	0.254
	Manning	0.715	1.086	0.454	0.812	0.658	0.336	0.756	0.819	0.354
39m	**Chezy**	0.700	0.852	0.430	0.926	0.380	0.225	0.863	0.514	0.252
	Manning	0.598	1.291	0.548	0.815	0.669	0.341	0.737	0.892	0.386
71m (65m)	**Chezy**	0.615	0.766	0.485	0.911	0.669	0.416	0.750	0.745	0.407
	Manning	0.524	1.098	0.603	0.816	0.983	0.535	0.685	0.999	0.490

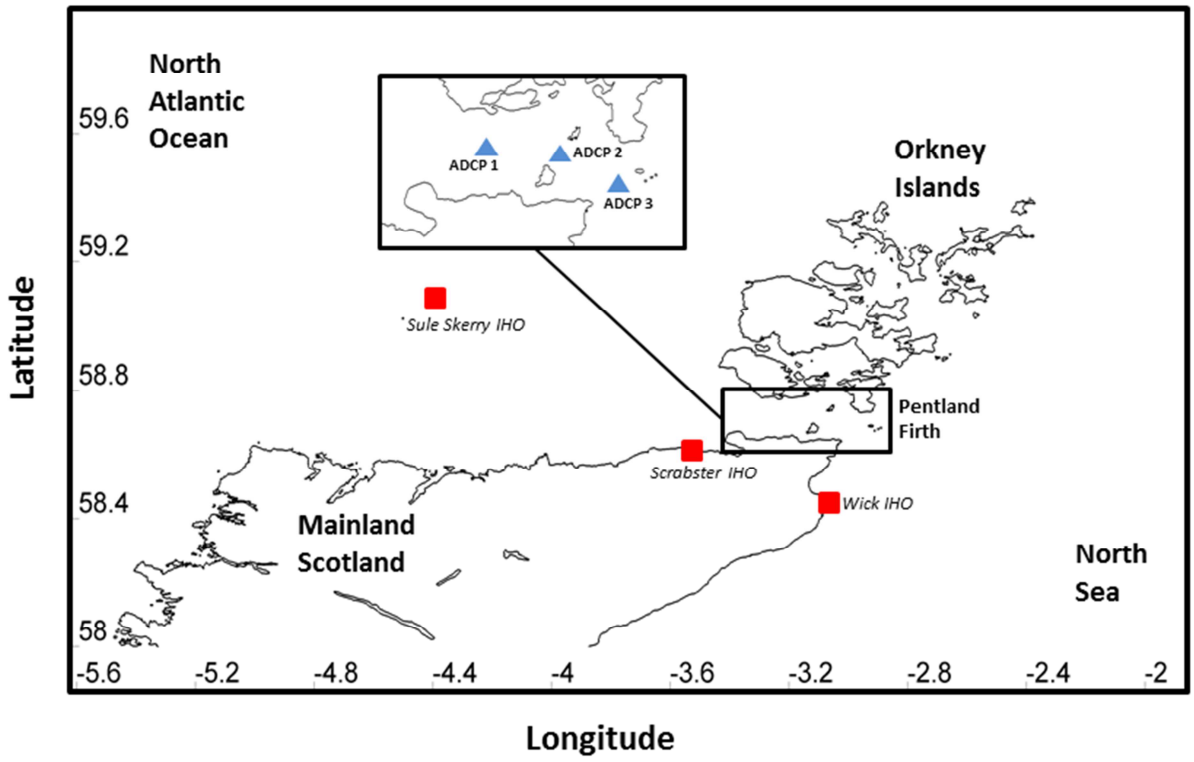

Figure 1: Map of the North of Scotland and Orkney Waters showing the location of the study area (Pentland Firth), including the position of the ADCPs (▲) and IHO tidal stations (■).

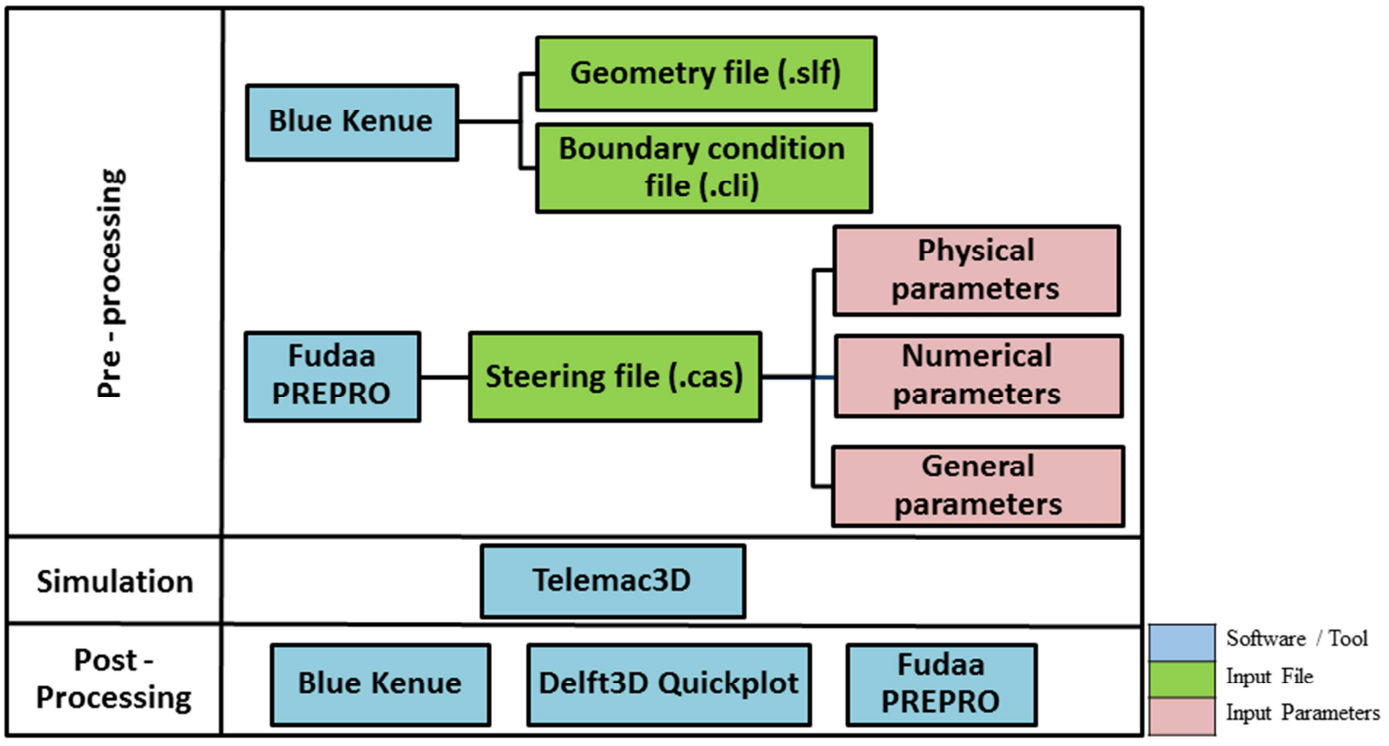

Figure 2: Process map for the development of a Telemac3D model.

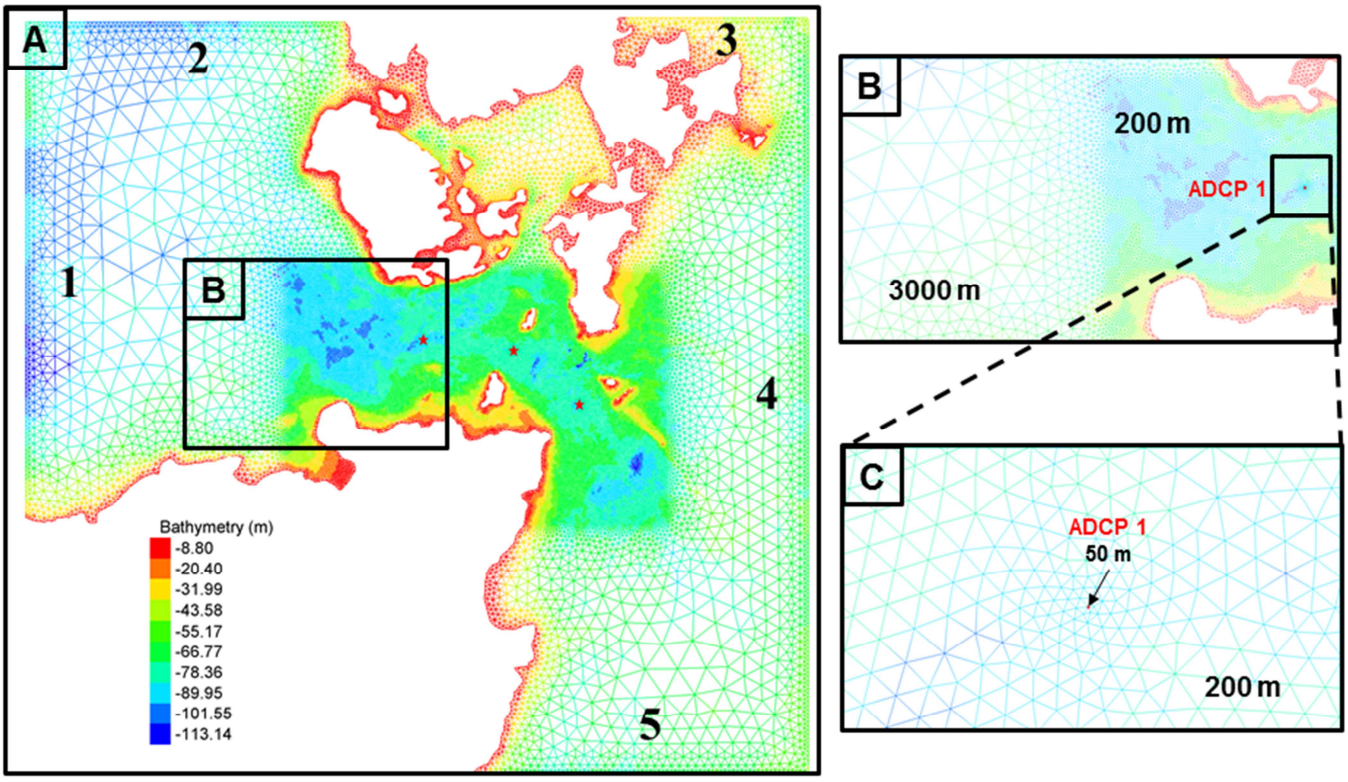

Figure 3: Computational domain used for the Telemac3D models, containing 285747 nodes and 497230 elements. (A) Mesh with the interpolated bathymetry. Number 1 till 5 corresponds to the liquid boundaries in the domain. (B) View of the coarser mesh resolution outside of the Pentland Firth, and the 200 m mesh density in the study area. (C) Hard point with 50 meter resolution at the monitoring station (ADCP location).

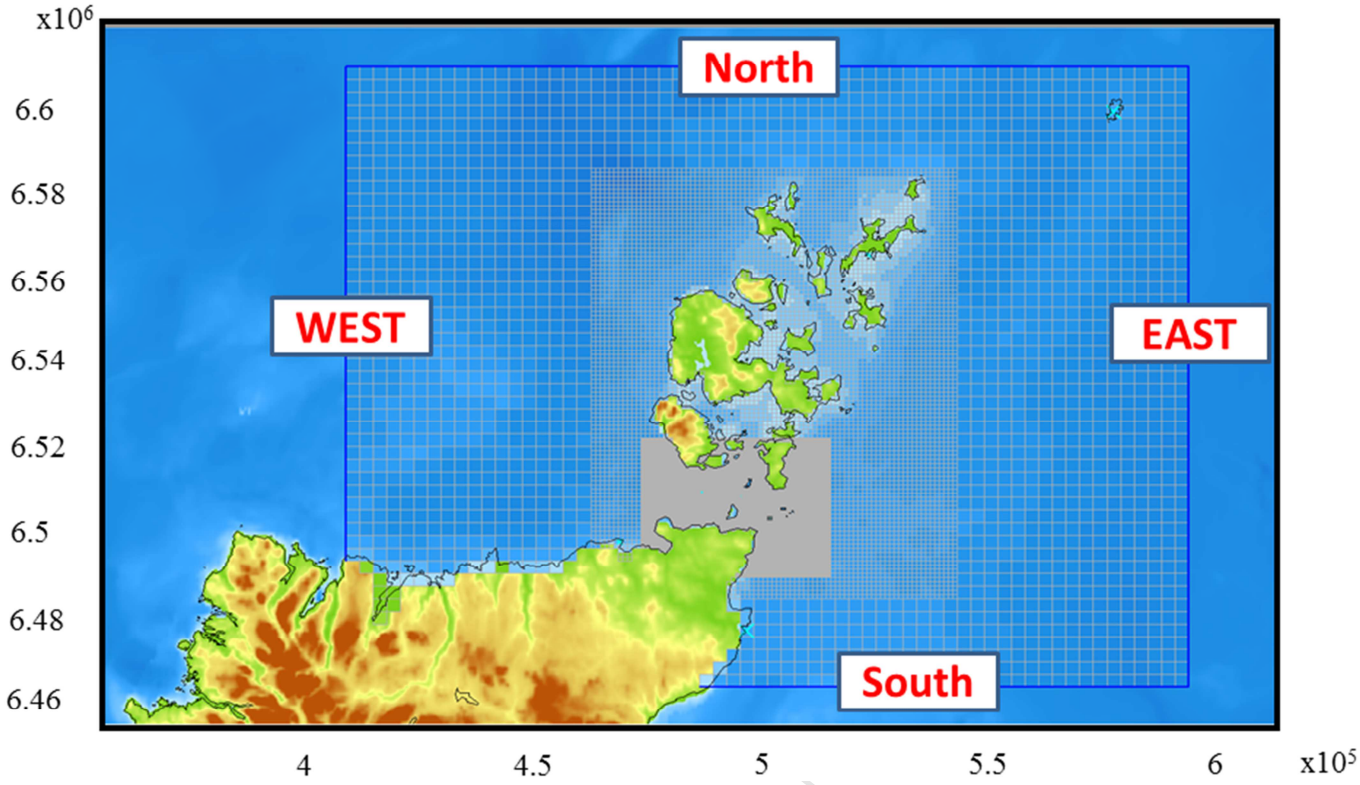

Figure 4: The computational domain and open boundary segments for the Delft3D model.

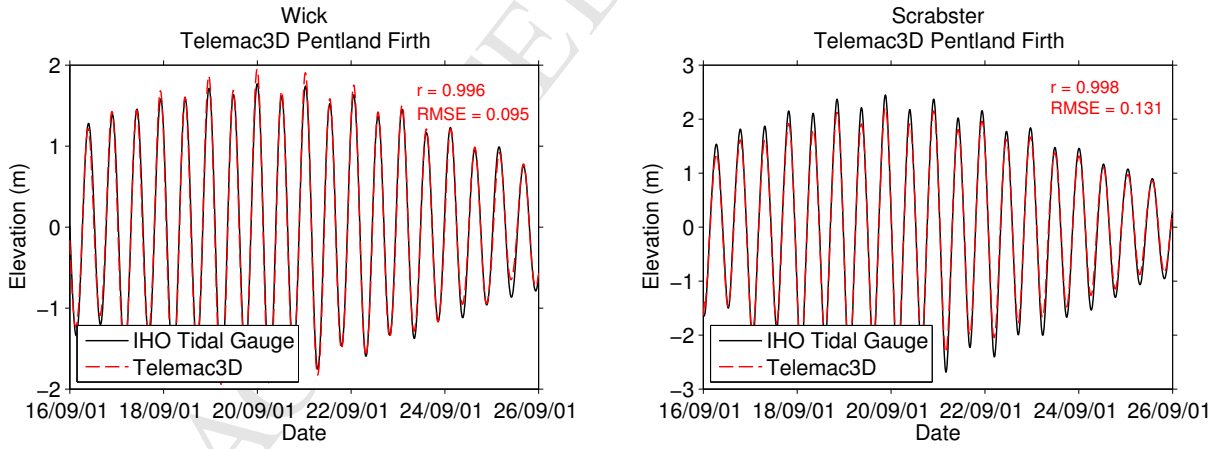

Figure 5: Comparison of the water surface elevation between the predicted and the measured data for the Telemac3D model. Left panel – Wick and right panel – Scrabster.

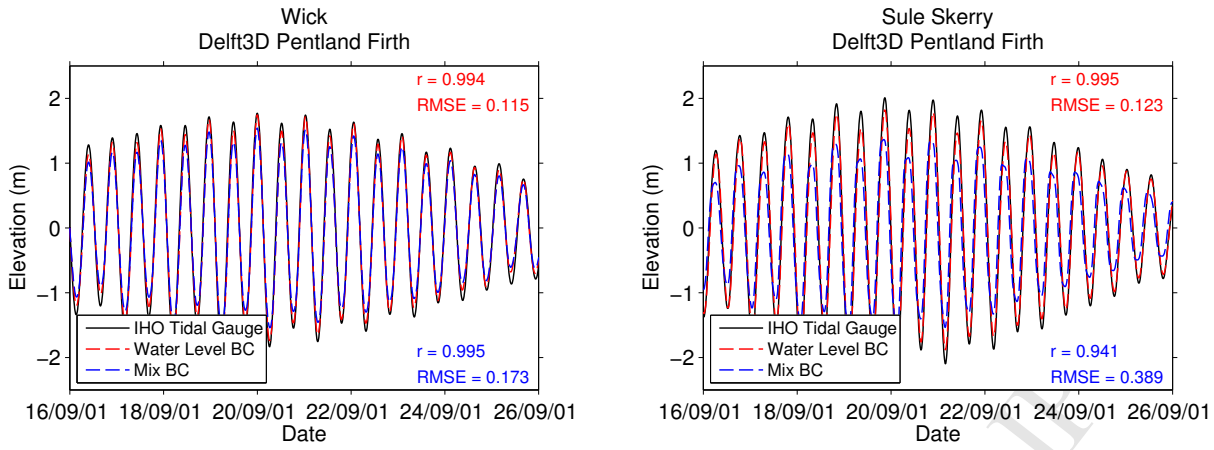

Figure 6: Comparison of the water surface elevation between the predicted and the measured data for the Delft3D model. Left panel – Wick and right panel – Sule Skerry.

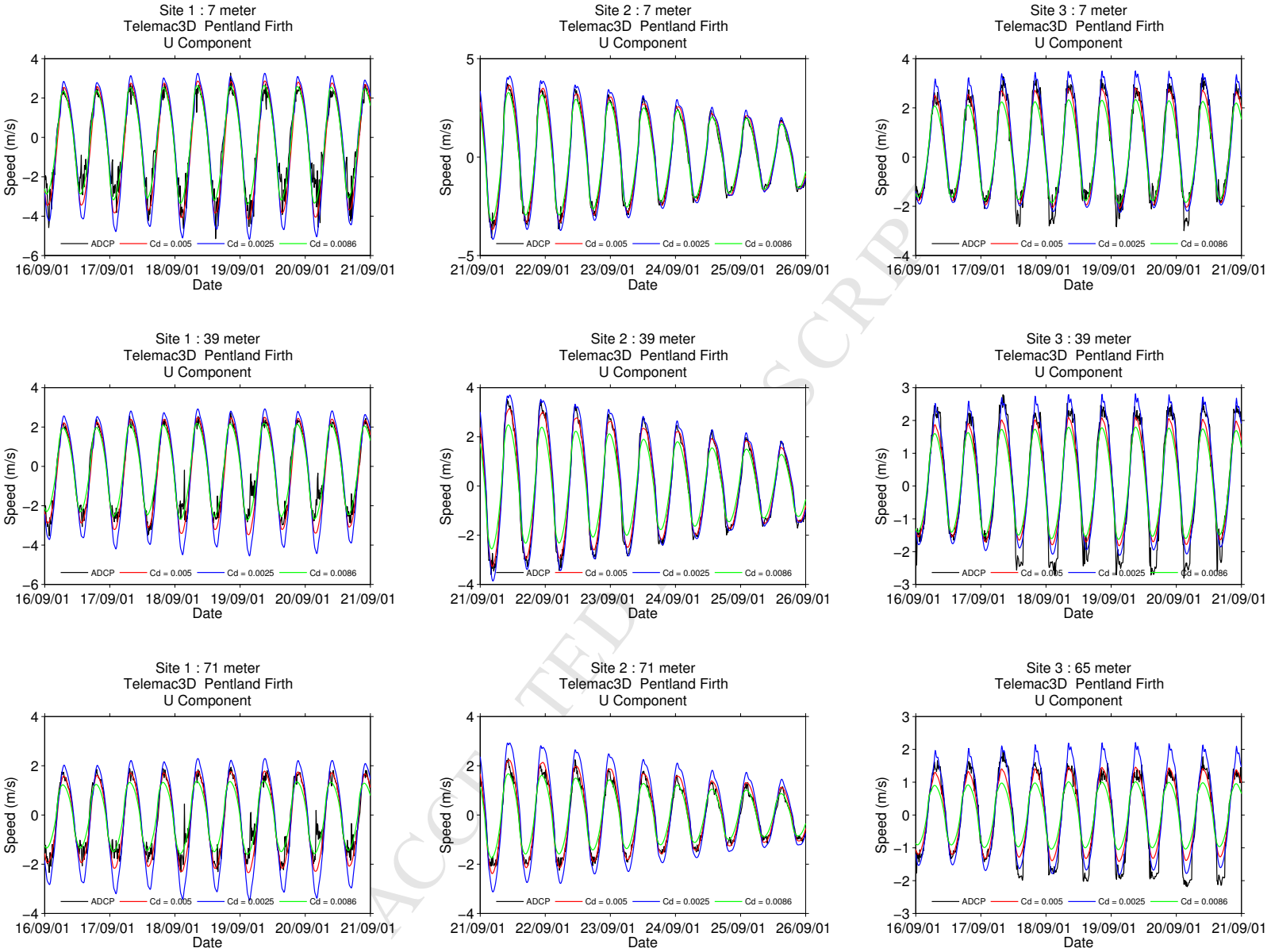

Figure 7: The influence of the roughness values [Cd = 0.005 (red line), 0.0025 (blue line), 0.0086 (green line)] on the U-velocity component for Telemac3D models.

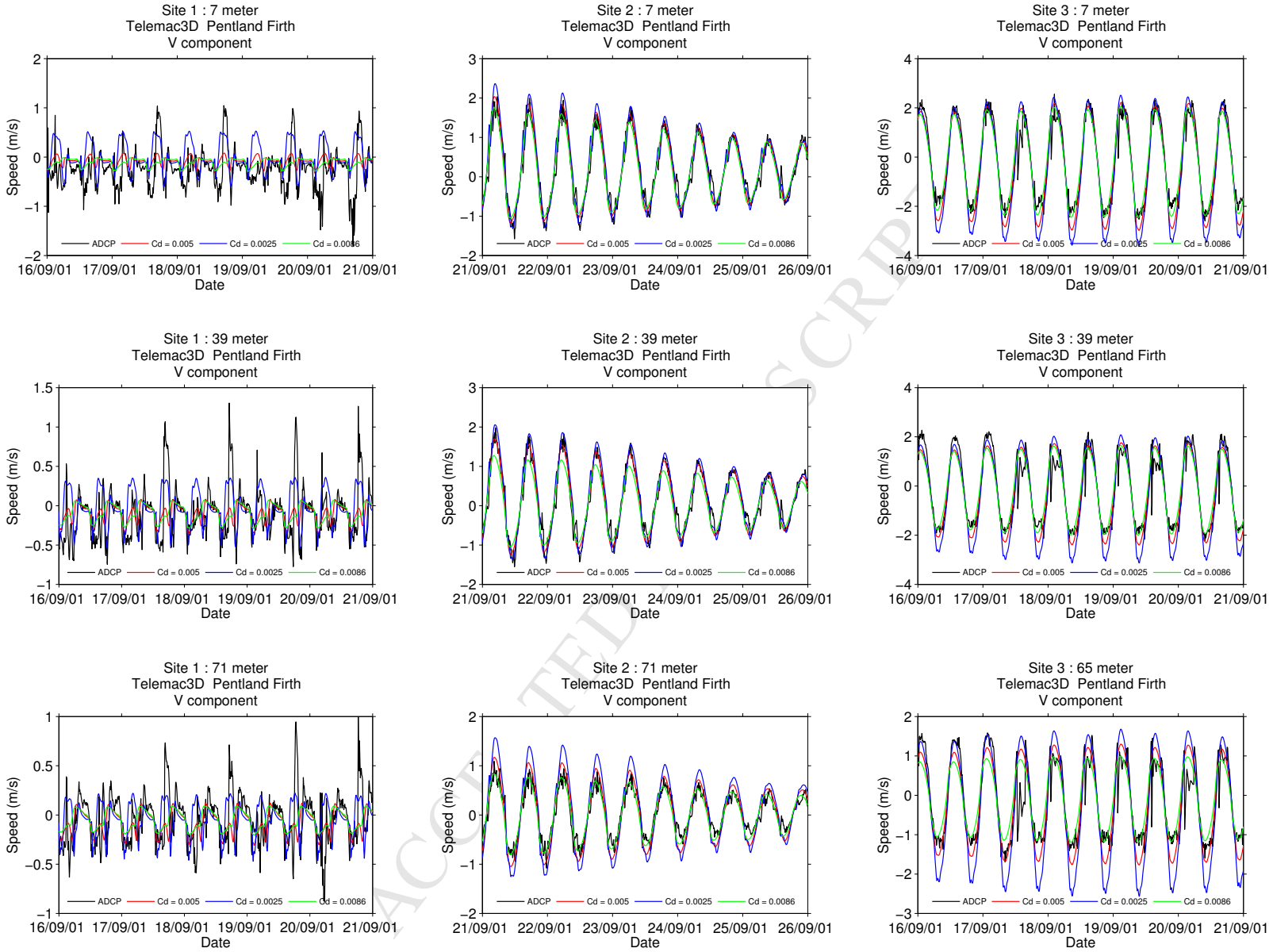

Figure 8: The influence of the roughness values [Cd = 0.005 (red line), 0.0025 (blue line), 0.0086 (green line)] on the V-velocity component for Telemac3D models.

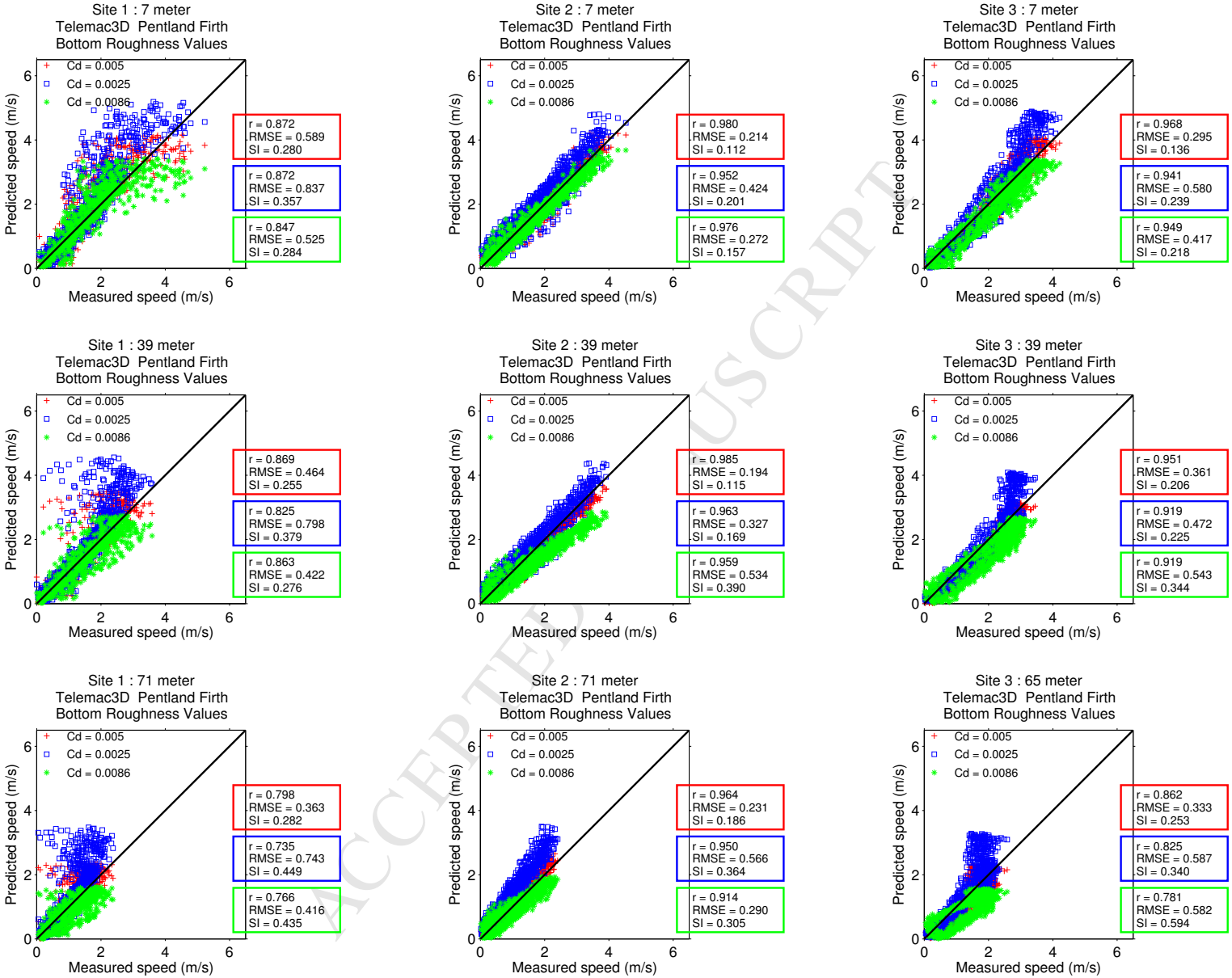

Figure 9: Scatter plots and the performance indices of three roughness values utilised in Telemac3D models at the three monitoring sites.

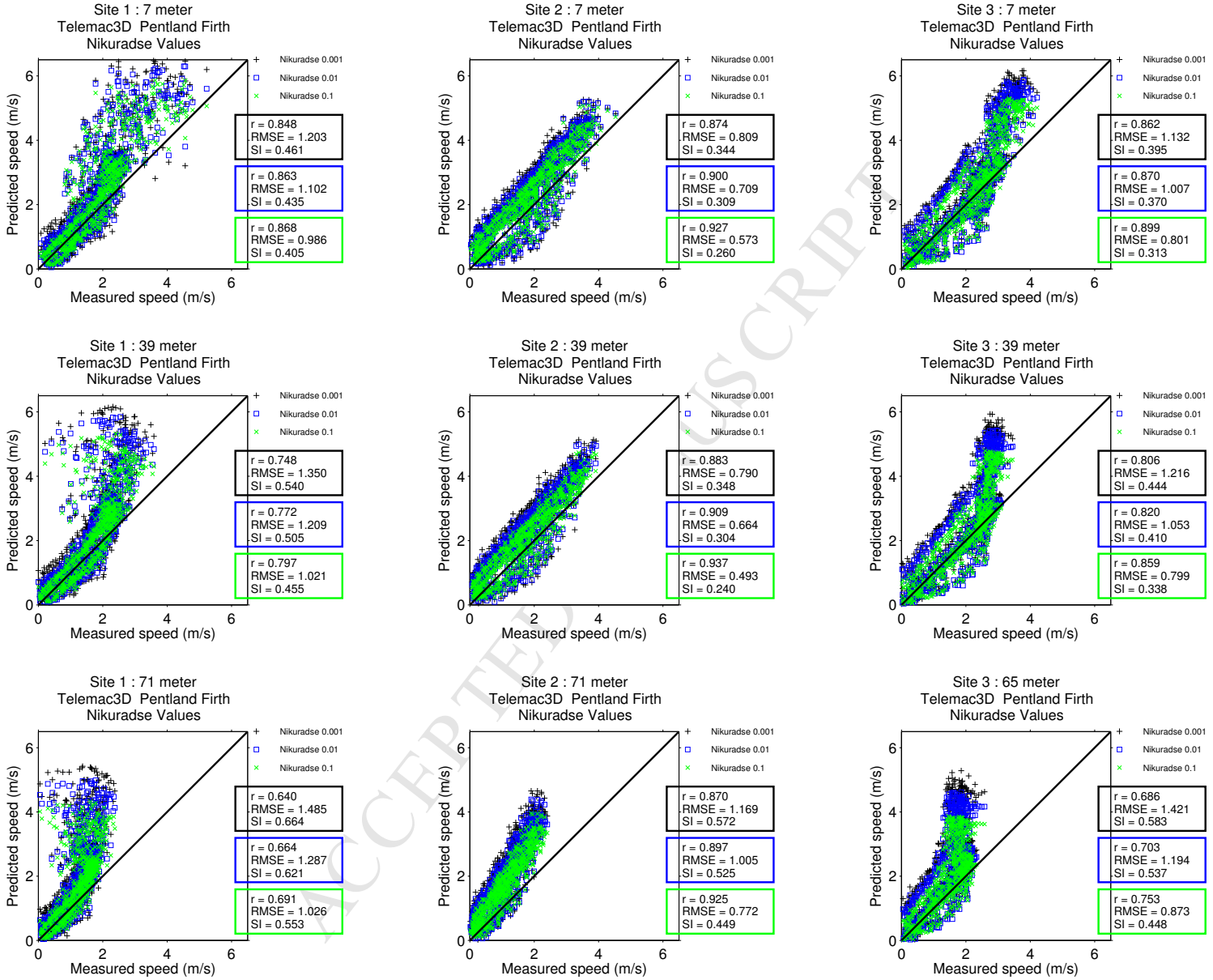

Figure 10: Comparison of several bottom roughness values using the Nikuradse formula on the Telemac3D models.

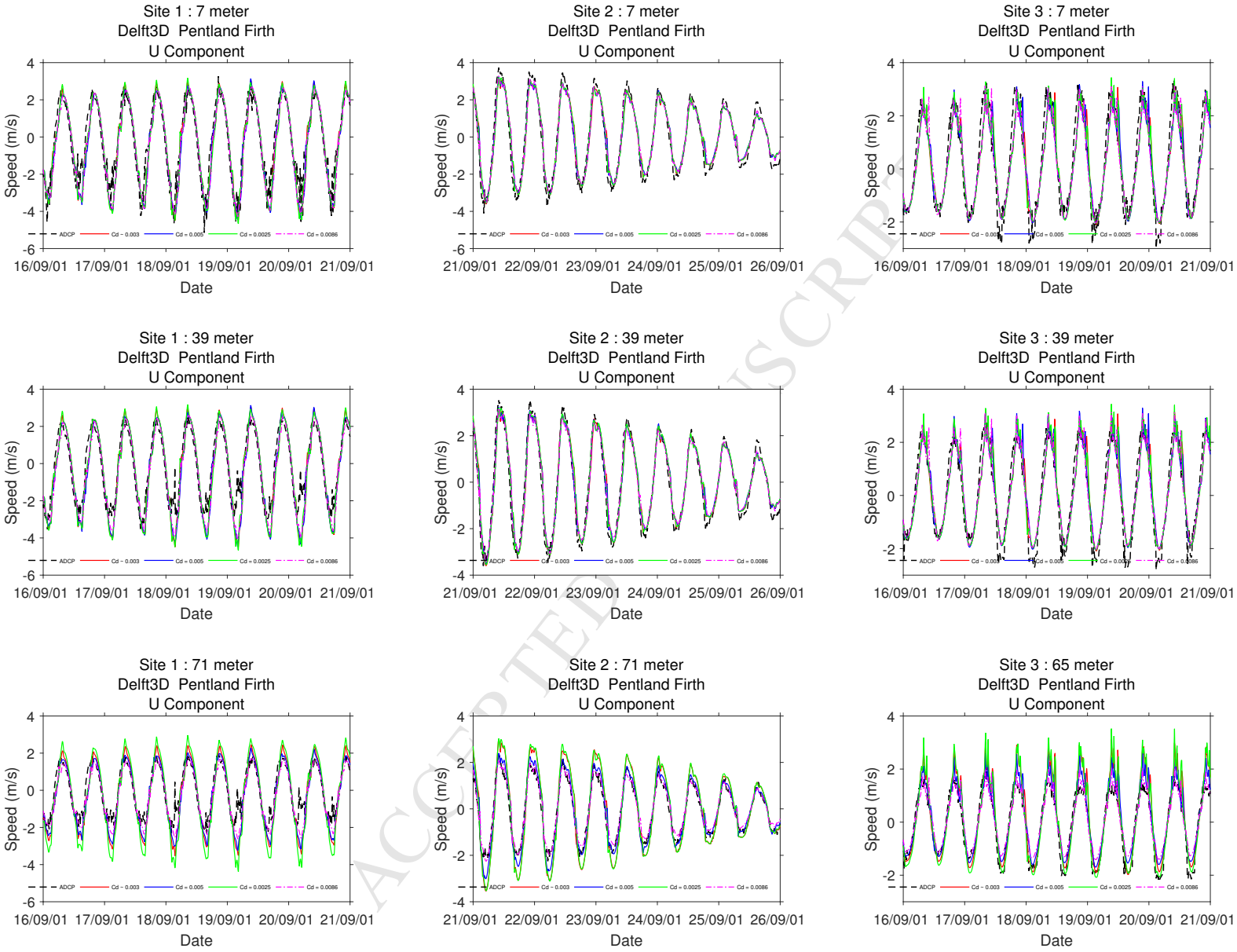

Figure 11: The influence of the roughness values on the U-velocity component for Delft3D models.

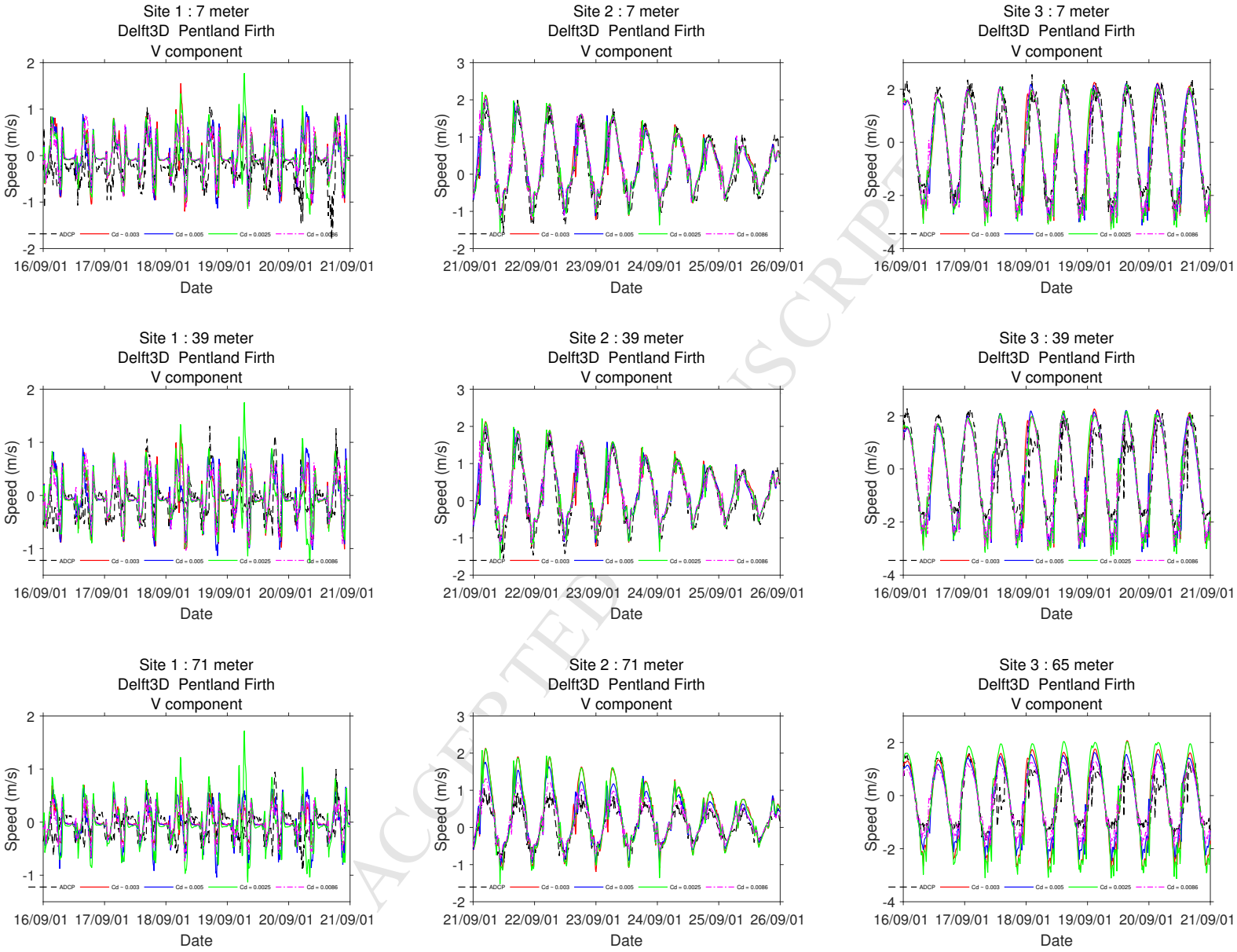

Figure 12: The influence of the roughness values on the V-velocity component for Delft3D models.

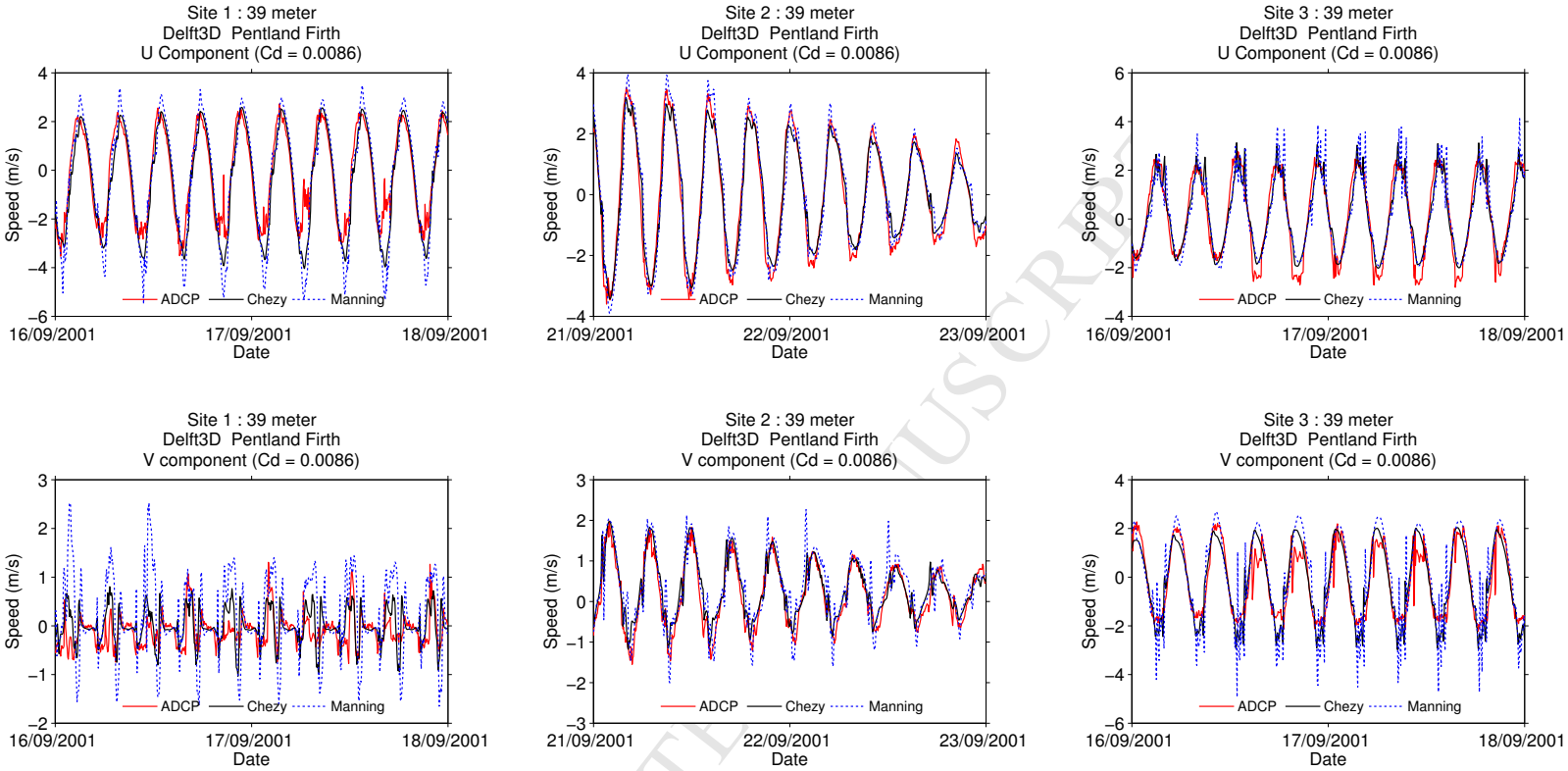

Figure 13: The velocity components at the mid water column using the Manning and Chezy bottom roughness formula for Delft3D models.